Nutrient starvation decreases Cx43 levels and limits intercellular communication in primary bovine corneal endothelial cells

Catheleyne D'hondt1*, Jegan Iyyathurai1*, Kirsten Welkenhuyzen1, Bernard Himpens1, Luc Leybaert2, Geert Bultynck1#

1 KU Leuven, Laboratory of Molecular and Cellular Signaling, Department of Cellular and Molecular Medicine, Campus Gasthuisberg O/N-I bus 802, Herestraat 49, BE-3000 Leuven, Belgium

2 Ghent University, Department of Basic Medical Sciences, Physiology Group, Faculty of Medicine and Health Sciences, BE-9000 Ghent, Belgium

* These authors have contributed equally to the study.

Correspondence to:

Geert Bultynck
Laboratory of Molecular and Cellular Signaling,
Department Cellular and Molecular Medicine
Campus Gasthuisberg O/N-I bus 802, Herestraat 49
BE-3000 Leuven, Belgium
geert.bultynck@med.kuleuven.be, +32-16-330215 (tel), +32-16-345991 (fax)

Abstract

Connexin (Cx) proteins form large conductance channels which function as regulators of communication between neighboring cells via gap junctions and/or hemichannels. Intercellular communication is essential to coordinate cellular responses in tissues and organs, thereby fulfilling an essential role in the spreading of signaling, survival and death processes. Connexin 43 (Cx43), a major connexin isoform in brain and heart, is rapidly turned-over. Recent studies implicated that autophagy, a lysosomal degradation pathway induced upon nutrient starvation, mediates connexins, including Cx43, degradation. Here, we examined the impact of nutrient starvation on endogenous Cx43-protein levels and endogenous Cx43-driven intercellular communication in primary bovine corneal endothelial cells (BCECs). Hank's Balanced Salt Solution (HBSS) was used as a starvation condition that induces autophagic flux without impacting the survival of the BCECs. Nutrient starvation of BCECs caused a rapid decline in Cx43-protein levels, both as gap junctions and as hemichannels. The time course of the decline in Cx43-protein levels coincided with the time course of the decline in intercellular communication, assessed as intercellular Ca^{2+}-wave propagation in BCECs exposed to a single-cell mechanical stimulus. The decline in Cx43-protein levels, both as gap junctions and as hemichannels, could be prevented by the addition of bafilomycin A1, a lysosomal inhibitor, during the complete nutrient starvation period. Consistent with this, bafilomycin A1 significantly alleviated the decrease in intercellular Ca^{2+}-wave propagation. This study further underpins the importance of autophagy as an important degradation pathway for Cx43 proteins during periods of nutrient deprivation, thereby impacting the ability of cells to perform intercellular communication.

Keywords

Starvation; autophagy; connexins

Introduction

Connexin 43 (Cx43) is one of the major connexin (Cx) isoforms expressed in a variety of tissues and organs, including the heart and the brain (Kar et al., 2012; Nielsen et al., 2012). Cx43 mediate intercellular communication by assembling into hexameric units that form i) head-to-head docked gap junction channels allowing direct chemical and electrical coupling between neighboring cells and ii) hemichannels allowing paracrine signaling networks by mediating the release of low molecular weight signaling molecules, including ATP and glutamate (Evans, De Vuyst & Leybaert, 2006; Herve & Derangeon, 2013; Scemes, Spray & Meda, 2009). The functional properties of these Cx43-based channels are tightly controlled by post-translational modification, interactions with other proteins and intramolecular interactions (D'Hondt et al., 2013b; Herve et al., 2012; Iyyathurai et al., 2013; Johnstone et al., 2012). Furthermore, Cx43-based channels are relatively short living due to their rapid turnover (Laing et al., 1997). Different processes have been implicated in the turnover of Cx43 gap junctions with prominent roles for the proteasomal, endo-/lysosomal and the autophago-/lysosomal (or autophagy) (Falk et al., 2012; Su, Cochrane & Lau, 2012). Autophagy is a catabolic process responsible for the turn-over of different cellular components and macro-molecules, including long-lived proteins, protein aggregates and damaged organelles (Feng et al., 2014). The process is executed by a set of autophagy-dependent genes (Atg), leading to the formation of autophagosomes, double-layered organelles that arise from ER-mitochondrial contact sites and accumulate these cellular components. Autophagosomes eventually fuse with the lysosomes, where these components are degraded and breakdown products are released back in the cytoplasm. Autophagy is tightly linked to the metabolic state of cells (Galluzzi et al., 2014). At the molecular level, autophagic flux is increased upon inhibition of the activity of the mammalian target of rapamycin (mTOR) and upon activation of the AMP-dependent kinase (AMPK) (Yang & Klionsky, 2010). As such, nutrient starvation and rapamycin, a chemical inhibitor of mTOR, are potent triggers of

autophagic flux. One of the methods to monitor autophagic flux is via an immunoblotting-based analysis of the lipidated form of LC3 (i.e. LC3-II) in the absence and presence of lysosomal inhibitors, like bafilomycin A1, which inhibits lysosomal function by targeting the V-type ATPase (Klionsky et al., 2012). Over recent years, there is accumulating evidence that autophagy accounts for the increased degradation of Cx43 (but also other Cx isoforms) gap junctions in response to nutrient starvation (Lichtenstein et al., 2011).

In this study, we exploited primary bovine corneal endothelial cells (BCECs) to study the impact of nutrient starvation on Cx43-driven intercellular communication by assessing intercellular Ca^{2+}-wave spreading in response to mechanical stimulation of a single cell (D'Hondt, Himpens & Bultynck, 2013a). BCECs endogenously express Cx43 proteins, which function both as gap junctions and hemichannels (D'Hondt et al., 2014). Cx43 is the major determinant of intercellular Ca^{2+}-wave spreading in these cells, because BCECs treated with siRNA against Cx43 displayed a more than 60% reduction in intercellular Ca^{2+}-wave spreading (Ponsaerts et al., 2010). As such, BCECs are a model system for assessing the molecular and functional regulation of Cx43 (D'Hondt et al., 2013a). Here, we show that endogenous Cx43 levels rapidly declined in cells undergoing autophagy by exposure to nutrient starvation, resulting in reduced intercellular communication. As a consequence, inhibiting lysosomal degradation using Bafilomycin A1 during nutrient starvation restored Cx43-protein levels and enhanced intercellular Ca^{2+}-wave propagation.

MATERIALS AND METHODS

Chemicals

Dulbecco's Modified Eagle's Medium (11960-044; Thermo Fisher Scientific), fetal bovine serum (F7524; Sigma-Aldrich), GlutaMAX™ (35050-038; Thermo Fisher Scientific), antibiotic-antimycotic mixture (15240-096; Thermo Fisher Scientific) and amphotericin-B (15290-026; Thermo Fisher Scientific), Fluo-4, AM (F14217; Thermo Fisher Scientific) and bafilomycin A1 (B-1080; LC laboratories). For Western blotting, the following antibodies were used: mouse monoclonal anti-GAPDH (G8795; Sigma-Aldrich), mouse monoclonal anti-β-Actin (A5441; Sigma-Aldrich), mouse monoclonal anti-Cx43 (C8093; Sigma-Aldrich), mouse monoclonal anti-LC3 (0231-100; nanoTools Antikörpertechnik GmbH and Co.) and rabbit monoclonal anti-PARP (9532S; Cell Signaling Technology).

Cell culture

Cultures of primary bovine corneal endothelial cells (BCECs) from fresh eyes were established as described previously (Gomes et al., 2005a; Gomes et al., 2005b; Gomes et al., 2006; D'Hondt et al., 2007a; D'Hondt et al., 2007b; Ponsaerts et al., 2008; Ponsaerts et al., 2010; D'hondt et al., 2009; Ponsaerts et al., 2012). The growth medium consisted of Dulbecco's Modified Eagle's Medium (DMEM), 10 % fetal bovine serum (FBS), 6.6 % GlutaMAX™, 1 % antibiotic-antimycotic mixture and 2.5 µg/ml amphotericin-B. Cells were grown at 37 °C in a humidified atmosphere containing 5 % CO_2. Cells of the first and second passages were harvested and seeded into two chambered glass slides (155380, Laboratory-Tek; Nunc, Roskilde, Denmark) at a density of 165,000 cells per chamber (4.2 cm^2). Cells were grown to confluence for three to four days before use. Except for data presented in Figure 1, nutrient starvation was performed by replacing the culture medium with Hank's Balanced Salt Solution (HBSS), as performed in

previous work from our lab for the study of autophagy (Decuypere et al., 2011). In Figure 1, nutrient starvation was also performed by using DMEM without FBS but with supplements (Glutamax, Amphotericin-B and Antibiotic/antimycotic) or by using DMEM without FBS and supplements. In all experiments, non-starved cells were used as the control condition (indicated as 0 hours starvation). Bafilomcyin A1 (100 nM) was added for the complete starvation period when studying Cx43 degradation. For determining autophagic flux, bafilomycin A1 (100 nM) was added 1 hour prior to harvesting the cells.

Imaging of intercellular Ca^{2+}-wave propagation

Intercellular Ca^{2+}-wave propagation was assayed in Fluo-4-loaded (10 µM for 30 min at 37 °C) BCECs as described previously (Gomes et al., 2005a; Gomes et al., 2005b; Gomes et al., 2006; D'Hondt et al., 2007a; D'Hondt et al., 2007b; Ponsaerts et al., 2008; Ponsaerts et al., 2010; D'hondt et al., 2009; Ponsaerts et al., 2012;). After washing the cells, the dye was excited at 488 nm, and its fluorescence emission was collected at 530 nm. Spatial changes in $[Ca^{2+}]_i$ following point mechanical stimulation were measured with the confocal microscope (LSM510) using a 40X objective (Air, 1.2 N.A.). A point mechanical stimulation, applied to a single cell, consisted of an acute deformation of the cell by briefly touching less than 1% percent of the surface area of its cell membrane with a glass micropipette (tip diameter <1 µm) coupled to a piezoelectric crystal (Piezo device P-280, Amplifier-E463; PI Polytech, Karlsruhe, Germany) mounted on a micro-manipulator, as described previously (Gomes et al., 2005a; Gomes et al., 2005b; Gomes et al., 2006; D'Hondt et al., 2007a; D'Hondt et al., 2007b; Ponsaerts et al., 2008; Ponsaerts et al., 2010; D'hondt et al., 2009; Ponsaerts et al., 2012;). We quantified the propagation of the intercellular Ca^{2+}-wave by measuring the total (maximal) surface area of responsive cells with a normalized ΔF of at least 1.1 (active area, AA), using imaging software (LSM Image 4.2; Zeiss). The AA is used as a quantitative measure for intercellular communication properties and is based on the activity of gap junctions and hemichannels. In BCECs, AA is mainly

determined by Cx43 hemichannels (major component) and Cx43 gap junctions (minor component) (D'Hondt et al., 2014). Further information about this approach can be found elsewhere (D'Hondt et al., 2013a).

Immunoblotting

BCECs were treated with lysis buffer containing 20 mM Tris-HCl pH 7.5, 150 mM NaCl, 1.5 mM $MgCl_2$, 0.5 mM DTT, 1 % Triton X-100, including a protease inhibitor cocktail (1 complete EDTA-free protease inhibitor tablet (Roche Applied Science) added per 50 ml). Lysate samples were subjected to SDS-PAGE (20 µg of protein per lane) using 12-well 4-12 % Bis/Tris gels (Thermo Fisher Scientific) and MES-running buffer (Thermo Fisher Scientific) and subsequent Western blotting after transfer to immobilon-P membranes (Millipore). In general, following dilutions of primary antibodies were used: anti-GAPDH at 1:50000; anti-β-Actin at 1:15000; anti-Cx43 at 1:1000; anti-LC3 at 1:500; anti-PARP at 1:500. HRP-conjugated secondary antibodies (Cell Signaling) were used at 1:2000. Detection was performed using Pierce ECL Western Blotting Substrate (Thermo Fisher Scientific) and the Chemidoc™ MP system (Bio-Rad, Nazareth Eke, Belgium). Since Cx43 and GAPDH/β actin have similar molecular weights, Cx43 and GAPDH/β actin immunoblots are typically obtained by running the same samples simultaneously on the same gel or on a different gel (dependent on the sample size), thereby staining one part of the gel or one gel with anti-Cx43 and one part of the gel or one gel with anti-GAPDH or anti-β actin.

Cell-surface biotinylation

The biotinylation experiment was performed according to the manufacturer's protocol (Pierce Cell Surface Protein Isolation Kit). Briefly, a monolayer of bovine corneal endothelial cells (90-95 % confluence) was cultured in T75 flasks and the cells were washed twice with ice-cold

Phosphate-buffered saline (PBS). 10 ml of biotin solution containing 0.25 mg/ml of sulfo-NHS-SS-biotin in PBS was added to each flask and incubated for 1 hour at 4 °C without shaking (2 flasks for each condition). Biotinylation reaction was stopped by adding quenching solution. After 5 min, the solution was removed and added 10 ml of Tris-buffered saline (TBS), which contains EDTA-free protease inhibitor (1 tablet per 50 ml). Subsequently, the cells from both flasks were scraped and pelleted in a conical tube by centrifugation (500*xg* for 5 min). The cells were lysed using 500 µl lysis buffer (10 mM Sodium phosphate, pH 7.2, 150 mM Sodium Chloride, 1.5 mM Magnesium Chloride, 1 % Triton X-100, 10 % glycerol and 10 µl/ml Halt™ Protease Inhibitor (Thermo Fisher Scientific)). Protein concentration of the lysates was determined by using BCA protein assays (Thermo Fisher Scientific) and equal amount of each conditions (1100 µg) were brought into 500 µl volume with lysis buffer. NeutrAvidin™ Agarose resin in total volume of 450 µl lysate and incubated overnight at 4 °C with end-over-end mixing. After this, the flow through fractions were collected and equal amounts were analysed by SDS-PAGE and subsequent immunoblotting. Beads were washed three times with washing buffer and biotinylated proteins were eluted from beads by 450 µl SDS-PAGE sample buffer containing DTT (62.5 mM Tris-HCl, pH 6.8, 1 % SDS, 10 % glycerol and 50 mM DTT) and allowed for 1 h at room temperature with end-over-end mixing. The eluted fractions were collected and equal amounts were analysed by SDS-PAGE and subsequent immunoblotting. Cx43 and GAPDH (negative control) antibodies were used for the Western-blotting procedure.

Apoptosis assay

The basic protocol for this analysis can be found elsewhere (Akl et al., 2013). Briefly, BCECs were washed with versene (Thermo Fisher Scientific) and trypsinized (0.05 % Trypsin-EDTA, Thermo Fisher Scientific) before starting the labeling. The cells were pelleted by centrifugation and gently resuspended in 100 µl Annexin V-binding buffer then 5 µl Annexin V-Alexa Fluor

488 (V13245, Thermo Fisher Scientific) and 2 µl 7-AAD (S10274, Thermo Fisher Scientific) was added. The samples were incubated at room temperature in the dark for 15 min and after this, 400 µl of Annexin V-binding buffer was added. Cell suspensions were analyzed by using the Attune NxT Flow Cytometer (Thermo Fisher Scientific). Flow cytometric data were plotted and analyzed using Attune cytometric software version 2.1.0.

Statistical analysis

All values represent mean +/- S.E.M. For statistical analyses, each treatment was compared to its respective control (i.e. 0 hours starvation) unless otherwise mentioned and significance was determined using a 1-way ANOVA. Differences were considered significant at $P < 0.05$. "N" indicates the number of days of experiments, while "n" represents the total number of independent experiments (the number of mechanically stimulated cells).

RESULTS

Starvation conditions impact Cx43-protein levels in primary BCECs

Here, we used primary BCECs for studying the impact of nutrient starvation, a major form of metabolic stress that induces autophagy, on the levels of native Cx43 channels. Therefore, we compared DMEM with FBS and supplements (+/+) to three independent starvation conditions applied for 4 hours, i.e. DMEM without FBS but with supplements (+/-), DMEM without FBS and supplements (-/-) and HBSS medium. All three starvation conditions tended to decrease the Cx43-protein levels, which could be restored by application of bafilomycin A1 during the complete starvation period (Fig. 1). However, the decline in Cx43-protein levels appeared to be more prominent in cells exposed to HBSS. This condition was chosen for further detailed experimental analysis.

Next, we performed a detailed analysis of the autophagy and cell death response of BCECs exposed to HBSS in the absence and presence of lysosomal inhibitors. We first determined that 4 hours of HBSS treatment was causing autophagic flux in primary BCECs by monitoring LC3-II levels in control conditions (normal medium; 0 hours starvation) and 4 hours HBSS treatment (Fig. 2a). From this analysis, it is clear that LC3-II levels are increased by exposing BCECs to HBSS and this increase is also observed in the presence of bafilomycin A1. Next, we also wished to perform a more detailed analysis of cell death in BCECs exposed to HBSS and lysosomal inhibitors. Therefore, we labeled BCECs with Annexin V-Alexa Fluor 488 (a marker for apoptosis) and 7-AAD (a marker for necrosis) and performed a flow cytometry analysis (Fig. 2b and Fig. 2c). These experiments indicate that cell survival of BCECs is not affected by any of these conditions, fully in line with previous observations made in our lab in different other cell lines exposed to HBSS for several hours (Decuypere JP et al, Autophagy, 2011). This indicates that exposing BCECs to HBSS for 4 hours is activating autophagy without impacting

cell survival, allowing a detailed analysis of studying the impacting of starvation by HBSS on Cx43-protein levels and function.

Starvation induces a time-dependent decrease of the Cx43-protein level

We first monitored Cx43-protein levels in total lysates of BCECs from normal medium (i.e. control condition; 0 hours starvation) exposed to different nutrient starvation periods, including 1.5, 4 and 6 hours of HBSS exposure, revealing a prominent, rapid and time-dependent decline in the total Cx43 protein levels (Fig. 3a). Quantification of the Cx43 signal over the GAPDH signal shows a significant reduction of Cx43 in starved cells versus non-starved cells (Fig. 3b). The signal in total lysates obtained from non-starved (0 hours starvation) cells was set at 100 % and the other values are relative to this. Using a surface biotinylation approach, we also determined whether both the levels of Cx43 gap junctions (i.e. the flow through (FT) fraction) and hemichannels (i.e. the elution fraction) declined upon nutrient starvation. The Cx43 immunoblots presented in Fig. 4a indicate that the levels of total Cx43, Cx43 gap junctions and Cx43 hemichannels decline in a time-dependent manner upon nutrient starvation of primary BCECs. Importantly, the immunoblots displaying GAPDH, a cytosolic protein, serve as an experimental control to verify that only surface proteins, but not intracellular proteins, are biotinylated (Fig. 4b).

Starvation induces a time-dependent in mechanical stimulation-induced intercellular communication

We previously established that knocking down Cx43 in BCEC caused a more than 60% reduction in the intercellular communication, measured as the active area of the intercellular Ca^{2+}-wave propagation in BCEC monolayers elicited by mechanical stimulation of a single cell (Ponsaerts et al., 2010). This indicated that Cx43 is the major connexin responsible for

intercellular communication in BCECs. Here, we assessed the impact of the different nutrient starvation periods on mechanical stimulation-induced intercellular communication. For all conditions used, the number of cells present in the imaging field was similar. Fig. 5a shows a typical Ca^{2+}-wave experiment before the mechanical stimulation, at the moment of mechanical stimulation and at the moment the maximal active area has been reached in non-starved cells and cells undergoing 4 hours of starvation. Fig. 5b shows the quantification of the maximal active area in non-starved cells (0 hours) and cells exposed to nutrient starvation for different time periods (1.5 hours, 4 hours and 6 hours). Consistent with the time-dependent decline in Cx43-protein levels, the active area of the Ca^{2+}-wave spreading was reduced upon nutrient starvation displaying a similar time-dependent pattern, showing a significant decline in the active area already after 1.5 hours of starvation.

Lysosomal inhibition prevents Cx43 degradation, both as gap junctions and as hemichannels

Since autophagy is activated by nutrient starvation and previous reports have implicated autophagy being responsible for Cx43 turnover (Fong et al., 2012; Lichtenstein et al., 2011), we assessed whether blocking lysosomal degradation using bafilomycin A1 could prevent nutrient starvation-induced Cx43 degradation in primary BCECs. For these experiments, Bafilomycin A1 was added for the whole nutrient starvation period, i.e. 1.5 hours, 4 hours or 6 hours, respectively. The total Cx43-protein levels were monitored in lysates obtained from non-starved cells and cells exposed to nutrient starvation in the presence or absence of bafilomycin A1 (Fig. 6). These immunoblots indicate that the decline of the Cx43-protein levels could be reversed by the lysosomal inhibitor bafilomycin A1. Next, we examined whether the degradation of both Cx43 gap junctions and hemichannels was prevented by bafilomycin A1. Therefore, we performed surface biotinylation experiments on control cells, cells exposed to 4 hours of nutrient starvation and cells exposed to 4 hours of nutrient starvation in the presence

of bafilomycin A1. Consistent with our previous experiment, the starvation-induced decrease in total Cx43-protein levels could be restored by the presence of bafilomycin A1 (Fig. 7a, upper panel). We also performed a surface-biotinylation experiment and western blot using anti-Cx43 antibodies in order to not only assess the total Cx43-protein levels, but also the levels of Cx43 gap junctions and of Cx43 hemichannels (Fig. 7a, middle and lower panel). Again, the cytosolic GAPDH served as an experimental control (Fig. 7b). In non-starved cells, it is clear that Cx43 immunoreactivity is present in both the FT and the eluted fraction (Fig. 7a). The latter represents the *bona fide* surface available fraction, since GAPDH immunoreactivity is only present in the FT but not in the eluted fraction (Fig. 7b). Consistent with the activation of autophagy upon nutrient starvation, addition of bafilomycin A1, a lysosomal inhibitor, for the complete starvation time period (4 hours) prevents the degradation of Cx43, both as gap junctions and as hemichannels.

The starvation-induced decrease in Cx43-driven intercellular communication can be partially rescued by bafilomycin A1.

Since the decrease in Cx43-protein levels triggered by starvation can be restored by the addition of bafilomycin A1, we aimed to investigate the impact of bafilomycin A1 on Cx43-driven intercellular Ca^{2+}-wave propagation induced by the mechanical stimulation of a single cell (Fig. 8). While 4 hours of nutrient starvation caused a prominent and significant decline in the mechanical stimulation-induced intercellular Ca^{2+}-wave propagation (quantified as the active area), addition of bafilomycin A1 during the nutrient-starvation period significantly prevented the reduction in active area. The active area of the Ca^{2+}-wave propagation remained lower than that of non-starved cells. This suggests that some Cx43 channels, though not being degraded by the lysosomes, may not be active or may be internalized and thus would not be available for providing intercellular communication.

Discussion

The major finding of this study is that the protein levels of endogenous Cx43 proteins are susceptible to metabolic stress, like triggered during periods of nutrient starvation. These conditions lead to a rapid decline in Cx43-protein levels, both at the gap junctional and hemichannel level, thereby negatively impacting the ability of Cx43 to drive intercellular communication in primary cell systems, like the BCECs. The degradation of Cx43, either as a gap junction or a hemichannel, likely occurs via autophagy, because i) the time-dependent decline in Cx43-protein levels correlated with the increase in LC3-II, an autophagic marker, when lysosomes were inhibited using bafilomycin A1, and ii) inhibition of lysosomal degradation, the final step in autophagy, during the nutrient starvation period restored Cx43-protein levels. As a consequence, lysosomal inhibition largely prevented the decline in intercellular communication in BCECs exposed to nutrient starvation. This shows that autophagy induction is an important pathway responsible for the turnover of endogenous Cx43 in BCECs in response to metabolic stress. This study supports earlier reports showing that connexins, and in particular Cx43, undergo autophagic degradation via the lysosomes in nutrient-starved cells (Bejarano et al., 2012; Carette et al., 2015; Fong et al., 2012; Hesketh et al., 2010; Lichtenstein et al., 2011). This further underpins the emerging concept that autophagy is responsible for Cx degradation, in particular during metabolic stress conditions, thereby limiting intercellular communication (Falk et al., 2012; Su et al., 2012; Su & Lau, 2014).

In cells, connexins are continuously recycled and are rapidly turned over. Seminal work by Beyer and his group indicated that Cx43 gap junctions are degraded via the ubiquitin-dependent proteasomal system (Laing & Beyer, 1995) and the lysosomal system (Laing et al., 1997). More recent studies have revealed a prominent role for autophagy as the major lysosomal degradation of connexin proteins, in particular during periods of nutrient starvation (Bejarano et al., 2012; Fong et al., 2012; Hesketh et al., 2010; Lichtenstein et al., 2011). The levels of Cx50 and Cx43

were found to rapidly decrease in response to autophagy-inducing conditions, like nutrient starvation (Lichtenstein et al., 2011). This observation suggests that autophagy is not selective for Cx43, but can also mediate the degradation of other Cx isoforms. Consistent with this, Cx50 colocalized with LC3, an autophagic marker and starvation-induced Cx50 degradation could be (partially) counteracted by chloroquin, another lysosomal inhibitor or by knocking down ATG5, an essential autophagy gene. Interestingly, Cx50P88S, a cataract-linked mutant form of Cx50, accumulates in the cytoplasm as punctae that are positively stained for LC3 and p62 and can be degraded by autophagy in response to nutrient starvation. These studies underpin previous microscopic observations of Cx43 in failing ventricular myocardium (Hesketh et al., 2010). In these conditions, Cx43 appears at the lateral membranes of cardiomyocytes and becomes heavily internalized by incorporation in LC3-positive autophagosomes, resulting in its degradation. In follow-up work (Bejarano et al., 2012), the colocalization of Cx43 with autophagic markers, LC3-II and p62, in response to nutrient starvation was confirmed, while chemical inhibition or genetic inhibition of autophagy (using ATG7-knockout cells) prevented Cx43 degradation. In this study, it seemed that autophagy inhibition was less effective in protecting Cx32 or Cx26 from autophagic degradation, indicating that autophagy may not equally important for every Cx isoform (Bejarano et al., 2012). Hence, in starvation conditions, autophagy may be the main degradation pathway for Cx43, but not for Cx32 or Cx26. This also fits with a previous report showing that Cx43 declined more rapidly than Cx50 in response to nutrient starvation (Lichtenstein et al., 2011). Of note, the type of stress that leads to autophagy might be important and might differentially impact the turnover of Cx isoforms, because the decrease in Cx32 levels in pancreatic acinar cells exposed to low pH was mediated by autophagy (Reed et al., 2014).

Moreover, the sequence of events and factors controlling autophagic degradation of Cx43 gap junctions were identified, indicating that Cx43 ought to be ubiquitinylated via NEDD4, an E3

ubiquitin-protein ligase that links ubiquitin to its targets (Bejarano et al., 2012). Eps15 is then recruited to ubiquitinylated Cx43 gap junctions, which favors the recruitment of autophagic markers like LC3 and p62, mediating Cx43 gap junction internalization and autophagic degradation. Knockdown of Eps15 prevents the autophagic degradation of Cx43 gap junctions (Bejarano et al., 2012). The internalization of Cx43 gap junctions and degradation by the autophagic machinery and lysosomal system has also been directly monitored using Cx43 linked to GFP, thereby supporting the conclusions from previous studies (Fong et al., 2012). Finally, it is important to note that autophagy not only impacts the connexin levels, but that connexins also impact basal autophagic flux by suppressing autophagosome formation (Bejarano et al., 2014). Plasmalemmal connexins seem to constitutively downregulate autophagic flux by scaffolding autophagy-related proteins responsible for the earlier steps in autophagosome formation. During nutrient starvation, these autophagy-inhibitory connexin complexes are disassembled by the recruitment of Atg14. As such, connexins become susceptible for internalization and autophagic degradation, thereby causing the removal of autophagic inhibitors and the upregulation of autophagic flux.

The importance of increased connexin, including Cx43, turn-over during periods of nutrient starvation requires further study. In particular, connexins have been implicated in the spreading of cell death signaling and factors (Decrock et al., 2009; Decrock et al., 2011; Decrock et al., 2012; Vinken et al., 2012a; Vinken et al., 2012b). As such, decreasing connexins may serve as a survival strategy during starvation and autophagy induction. In addition, connexin hemichannels also mediate paracrine signaling via the release of ATP and glutamate (Wang et al., 2013). As such, decreasing connexin hemichannels during autophagy induction may be a cellular strategy to prevent the loss of energy molecules. Finally, impaired autophagy has been implicated in ageing conditions and several pathological conditions, including oncogenesis and neurodegeneration (Rubinsztein, Marino & Kroemer, 2011; Frake et al., 2015; Galluzzi et al.,

2015; Kroemer, 2015; Menzies, Fleming & Rubinsztein, 2015; Rubinsztein, Bento & Deretic, 2015). Enhancing autophagy using small molecules & compounds has been proposed as a therapeutic strategy (Kroemer, 2015; Rubinsztein et al., 2015). Now, defective turnover of connexins may contribute to these disease states. For instance, in the context of Alzheimer's disease, β-amyloid has been shown to cause neuronal death via the activation of glial Cx43 hemichannels and neuronal Cx36 and Panx1 hemichannels (Orellana et al., 2011). Similar "toxic" roles for astroglial and neuronal hemichannels have been observed in several inflammatory conditions, like induced by FGF-1, spinal cord injury or hypoxia and glucose deprivation (Bennett et al., 2012). Thus, stimulating autophagy in neurons and/or glial cells may be beneficial for neuronal survival in these conditions, thereby reducing Cx hemichannel levels and counteracting their "toxic" functions in response to β-amyloid or other inflammatory conditions. However, further work is required to elucidate whether molecules that induce autophagy, like the mTOR inhibitor rapamycin, too results in a decline of connexins as gap junctions and hemichannels and can counteract β-amyloid toxicity in neurons by promoting the degradation of connexin hemichannels.

In conclusion, we report that Cx43 proteins are rapidly degraded via autophagy, a lysosomal-turnover pathway, in cells exposed to metabolic stress, like nutrient starvation. This limits the ability of cells to establish physiological intercellular communication, like intercellular Ca^{2+}-wave propagation, via Cx43 gap junctions and/or hemichannels. Under such conditions, inhibition of autophagy might be beneficial to restore Cx43-protein levels and to partially rescue intercellular communication.

ACKNOWLEDGEMENTS

The work has been supported by the Research Foundation – Flanders (F.W.O.; grant G.0298.11 to LL and GB and G.0634.13 to GB), Interuniversity Attraction Poles Program (Belgian Science Policy; P7/13 to G.B and P7/10 to L.L.) and a "Krediet aan Navorser" grant of the FWO (15117.14N to CDH). We thank Dr. Jean-Paul Decuypere for advice and all group members for helpful discussions.

Figure legends

Fig. 1 Different starvation conditions decrease Cx43-protein levels in primary BCECs.
BCECs were treated with 4 different conditions (all in the absence or presence of 100 nM bafilomycin A1, added during the complete starvation period): DMEM with FBS and supplements (+/+), DMEM without FBS but with supplements (+/-), DMEM without FBS and supplements (-/-) and HBSS medium. Immunoblot analysis shows the Cx43 and β actin-protein levels. Densitometry values are shown for Cx43 over β-Actin, relative to the +/+ condition without bafilomycin A1, which was set at 1.

Fig. 2 Nutrient starvation (HBSS) induces autophagic flux without cell death in primary BCECs.
(a) Immunoblot analysis of LC3-II in BCECs from non-starved conditions (0h starvation) and starved conditions (4h starvation with HBSS). Autophagic flux was measured by the addition of bafilomycin A1 (100 nM; last 1 hour). Densitometry values are shown for LC3-II over β-Actin, relative to the 0h starvation condition without bafilomycin A1, which was set at 1. ***(b)*** Flow cytometry analysis of Annexin V-Alexa Fluor 488/7-AAD-stained BCECs from non-starved conditions (0h starvation) and starved conditions (4h starvation with HBSS) in absence and presence of bafilomycin A1 (100 nM; 4 hours). R2 gate represents the necrosis population, R3 gate represents the apoptotic population with secondary necrosis, R4 gate represents the living cell population and R5 gate represents the apoptotic population. ***(c)*** Bar graph showing the mean percentage of living cells (R4 population) obtained for the 4 different conditions.

Fig. 3 Nutrient starvation (HBSS) induces a time-dependent decline in the total Cx43-protein levels in primary BCECs.
(a) Lysates of BCECs exposed to different time periods of nutrient starvation were subjected to SDS-PAGE and Western blotting. A typical immunoblot stained with anti-Cx43 shows the time-dependent decrease of the Cx43 protein in lysates of BCECs exposed to different time periods of nutrient starvation (0 hours, 0h; 1.5 hours, 1.5h; 4 hours, 4h; 6 hours, 6h). An immunoblot stained with anti-GAPDH of the same samples but from different lanes of the same gel is also shown. ***(b)*** The bar graph shows the normalized Cx43-protein levels obtained from immunoblot analysis of lysates of BCECs starved for different time periods. The data indicate mean ± S.E.M. (N = 9). * indicates a statistical difference with the control condition (0h starvation).

Fig. 4 Nutrient starvation (HBSS) induces a time-dependent decline in the Cx43 gap junction and hemichannel fraction in primary BCECs.
(a) A representative immunoblot stained for Cx43 from a cell-surface biotinylation experiment shows the time-dependent decrease in total Cx43 levels (Lysate), Cx43-gap junction levels (flow through; FT) and Cx43-hemichannel levels (Elution). ***(b)*** The corresponding immunoblot of the exactly the same samples but stained for GAPDH, a cytosolic protein.

Fig. 5 Nutrient starvation (HBSS) induces a decline in intercellular Ca^{2+}-wave propagation in BCEC monolayers triggered by a single-cell mechanical stimulus.
(a) Representative pseudo-colored fluorescence images showing Ca^{2+} transients at different times after mechanical stimulation in control conditions and upon starvation in BCEC. The first image shows the fluorescence intensities before mechanical stimulation (MS). The second image shows the fluorescence intensities of the mechanically stimulated cell upon stimulation. The third image shows the maximal active area (AA). ***(b)*** The graph shows the normalized active area values obtained from BCECs exposed to different time periods of nutrient starvation. Data points indicate mean ± S.E.M. (N = 4, n = 40). * indicates a statistical difference with the control condition (0h starvation).

Fig. 6 The nutrient starvation (HBSS)-induced decline in total Cx43-protein levels in primary BCECs can be prevented by the addition of bafilomycin A1.
A representative experiment showing the levels of Cx43 and β-Actin in lysates obtained from non-starved (0 h) BCECs and nutrient starved BCECs, treated or not with bafilomycin A1. Nutrient starvation was done for 1.5, 4 and 6 hours. The decline of total Cx43-protein levels by nutrient starvation is prevented by the addition of bafilomycin A1. Densitometry values are calculated for Cx43 over β-Actin, relative to the 0h starvation condition without bafilomycin A1, which was set as 1.

Fig. 7 Bafilomycin A1 prevents the starvation (HBSS)-induced degradation of Cx43 gap junctions and hemichannels in BCECs.
(a) A representative cell-surface biotinylation experiment showing that bafilomycin A1 prevents the degradation of total Cx43 (lysate), Cx43 gap junctions (flow through; FT) and Cx43 hemichannels (Elution) induced nutrient starvation. Starvation in the absence or presence of bafilomycin A1 was induced for 4 hours. ***(b)*** The corresponding GAPDH levels obtained from the same samples as used for assessing Cx43 levels.

Fig. 8 Bafilomycin A1 partially alleviates the starvation (HBSS)-induced decrease in active area in BCECs.
The graph shows the normalized active area values obtained from BCECs exposed to mechanical stimulus in non-starved cells (0h starvation), nutrient starvation (4h starvation) and nutrient starvation combined with 100 nM bafilomycin A1 added for 4 hours. Data represent mean ± S.E.M. (N=3, n=30). * indicates a statistical difference with the control condition (0h starvation), while ^ indicates a statistical difference between 4h starvation conditions in the absence and presence of bafilomycin A1.

References

Akl, H, Monaco, G, La Rovere, R, Welkenhuyzen, K, Kiviluoto, S, Vervliet, T, Molgo, J, Distelhorst, CW, Missiaen, L, Mikoshiba, K, Parys, JB, De Smedt, H, Bultynck, G (2013). IP3R2 levels dictate the apoptotic sensitivity of diffuse large B-cell lymphoma cells to an IP3R-derived peptide targeting the BH4 domain of Bcl-2. Cell Death Dis 4:e632

Bejarano, E, Girao, H, Yuste, A, Patel, B, Marques, C, Spray, DC, Pereira, P, Cuervo, AM (2012). Autophagy modulates dynamics of connexins at the plasma membrane in a ubiquitin-dependent manner. Mol Biol Cell 23:2156-69

Bejarano, E, Yuste, A, Patel, B, Stout, RF, Jr., Spray, DC, Cuervo, AM (2014). Connexins modulate autophagosome biogenesis. Nat Cell Biol 16:401-14

Bennett, MV, Garre, JM, Orellana, JA, Bukauskas, FF, Nedergaard, M, Saez, JC (2012). Connexin and pannexin hemichannels in inflammatory responses of glia and neurons. Brain Res 1487:3-15

Carette, D, Gilleron, J, Denizot, JP, Grant, K, Pointis, G, Segretain, D (2015). New cellular mechanisms of gap junction degradation and recycling. Biol Cell

D'Hondt, C, Himpens, B, Bultynck, G (2013a). Mechanical stimulation-induced calcium wave propagation in cell monolayers: the example of bovine corneal endothelial cells. J Vis Exp:e50443

D'Hondt, C, Iyyathurai, J, Himpens, B, Leybaert, L, Bultynck, G (2014). Cx43-hemichannel function and regulation in physiology and pathophysiology: insights from the bovine corneal endothelial cell system and beyond. Front Physiol 5:348

D'Hondt, C, Iyyathurai, J, Vinken, M, Rogiers, V, Leybaert, L, Himpens, B, Bultynck, G (2013b). Regulation of connexin- and pannexin-based channels by post-translational modifications. Biol Cell 105:373-98

D'Hondt, C, Ponsaerts, R, Srinivas, SP, Vereecke, J, Himpens, B (2007a). Thrombin inhibits intercellular calcium wave propagation in corneal endothelial cells by modulation of hemichannels and gap junctions. Invest Ophthalmol Vis Sci 48:120-33

D'hondt, C, Ponsaerts, R, Srinivas, SP, Vereecke, J, Himpens, B (2009). Reduced intercellular communication and altered morphology of bovine corneal endothelial cells with prolonged time in cell culture. Curr Eye Res 34:454-65

D'Hondt, C, Srinivas, SP, Vereecke, J, Himpens, B (2007b). Adenosine opposes thrombin-induced inhibition of intercellular calcium wave in corneal endothelial cells. Invest Ophthalmol Vis Sci 48:1518-27

Decrock, E, Krysko, DV, Vinken, M, Kaczmarek, A, Crispino, G, Bol, M, Wang, N, De Bock, M, De Vuyst, E, Naus, CC, Rogiers, V, Vandenabeele, P, Erneux, C, Mammano, F, Bultynck, G, Leybaert, L (2012). Transfer of IP(3) through gap junctions is critical, but not sufficient, for the spread of apoptosis. Cell Death Differ 19:947-57

Decrock, E, Vinken, M, Bol, M, D'Herde, K, Rogiers, V, Vandenabeele, P, Krysko, DV, Bultynck, G, Leybaert, L (2011). Calcium and connexin-based intercellular communication, a deadly catch? Cell Calcium 50:310-21

Decrock, E, Vinken, M, De Vuyst, E, Krysko, DV, D'Herde, K, Vanhaecke, T, Vandenabeele, P, Rogiers, V, Leybaert, L (2009). Connexin-related signaling in cell death: to live or let die? Cell Death Differ 16:524-36

Decuypere, JP, Welkenhuyzen, K, Luyten, T, Ponsaerts, R, Dewaele, M, Molgo, J, Agostinis, P, Missiaen, L, De Smedt, H, Parys, JB, Bultynck, G (2011). Ins(1,4,5)P3 receptor-mediated Ca2+ signaling and autophagy induction are interrelated. Autophagy 7:1472-89

Evans, WH, De Vuyst, E, Leybaert, L (2006). The gap junction cellular internet: connexin hemichannels enter the signalling limelight. Biochem J 397:1-14

Falk, MM, Fong, JT, Kells, RM, O'Laughlin, MC, Kowal, TJ, Thevenin, AF (2012). Degradation of endocytosed gap junctions by autophagosomal and endo-/lysosomal pathways: a perspective. J Membr Biol 245:465-76

Feng, Y, He, D, Yao, Z, Klionsky, DJ (2014). The machinery of macroautophagy. Cell Res 24:24-41

Fong, JT, Kells, RM, Gumpert, AM, Marzillier, JY, Davidson, MW, Falk, MM (2012). Internalized gap junctions are degraded by autophagy. Autophagy 8:794-811

Frake, RA, Ricketts, T, Menzies, FM, Rubinsztein, DC (2015). Autophagy and neurodegeneration. J Clin Invest 125:65-74

Galluzzi, L, Pietrocola, F, Bravo-San Pedro, JM, Amaravadi, RK, Baehrecke, EH, Cecconi, F, Codogno, P, Debnath, J, Gewirtz, DA, Karantza, V, Kimmelman, A, Kumar, S, Levine, B, Maiuri, MC, Martin, SJ, Penninger, J, Piacentini, M, Rubinsztein, DC, Simon, HU, Simonsen, A, Thorburn, AM, Velasco, G, Ryan, KM, Kroemer, G (2015). Autophagy in malignant transformation and cancer progression. EMBO J 34:856-80

Galluzzi, L, Pietrocola, F, Levine, B, Kroemer, G (2014). Metabolic control of autophagy. Cell 159:1263-76

Gomes, P, Srinivas, SP, Van Driessche, W, Vereecke, J, Himpens, B (2005a). ATP release through connexin hemichannels in corneal endothelial cells. Invest Ophthalmol Vis Sci 46:1208-18

Gomes, P, Srinivas, SP, Vereecke, J, Himpens, B (2005b). ATP-dependent paracrine intercellular communication in cultured bovine corneal endothelial cells. Invest Ophthalmol Vis Sci 46:104-13

Gomes, P, Srinivas, SP, Vereecke, J, Himpens, B (2006). Gap junctional intercellular communication in bovine corneal endothelial cells. Exp Eye Res

Herve, JC, Derangeon, M (2013). Gap-junction-mediated cell-to-cell communication. Cell Tissue Res 352:21-31

Herve, JC, Derangeon, M, Sarrouilhe, D, Giepmans, BN, Bourmeyster, N (2012). Gap junctional channels are parts of multiprotein complexes. Biochim Biophys Acta 1818:1844-65

Hesketh, GG, Shah, MH, Halperin, VL, Cooke, CA, Akar, FG, Yen, TE, Kass, DA, Machamer, CE, Van Eyk, JE, Tomaselli, GF (2010). Ultrastructure and regulation of lateralized connexin43 in the failing heart. Circ Res 106:1153-63

Iyyathurai, J, D'hondt, C, Wang, N, De Bock, M, Himpens, B, Retamal, MA, Stehberg, J, Leybaert, L, Bultynck, G (2013). Peptides and peptide-derived molecules targeting the intracellular domains of Cx43: Gap junctions versus hemichannels. Neuropharmacology

Johnstone, SR, Billaud, M, Lohman, AW, Taddeo, EP, Isakson, BE (2012). Posttranslational modifications in connexins and pannexins. J Membr Biol 245:319-32

Kar, R, Batra, N, Riquelme, MA, Jiang, JX (2012). Biological role of connexin intercellular channels and hemichannels. Arch Biochem Biophys 524:2-15

Klionsky, DJ, Abdalla, FC, Abeliovich, H, Abraham, RT, Acevedo-Arozena, A, Adeli, K, Agholme, L, Agnello, M, Agostinis, P, Aguirre-Ghiso, JA, Ahn, HJ, Ait-Mohamed, O, Ait-Si-Ali, S, Akematsu, T, Akira, S, Al-Younes, HM, Al-Zeer, MA, Albert, ML, Albin, RL, Alegre-Abarrategui, J, Aleo, MF, Alirezaei, M, Almasan, A, Almonte-Becerril, M, Amano, A, Amaravadi, R, Amarnath, S, Amer, AO, Andrieu-Abadie, N, Anantharam, V, Ann, DK, Anoopkumar-Dukie, S, Aoki, H, Apostolova, N, Arancia, G, Aris, JP, Asanuma, K, Asare, NY, Ashida, H, Askanas, V, Askew, DS, Auberger, P, Baba, M, Backues, SK, Baehrecke, EH, Bahr, BA, Bai, XY, Bailly, Y, Baiocchi, R, Baldini, G, Balduini, W, Ballabio, A, Bamber, BA, Bampton, ET, Banhegyi, G, Bartholomew, CR, Bassham, DC, Bast, RC, Jr., Batoko, H, Bay, BH, Beau, I, Bechet, DM, Begley, TJ, Behl, C, Behrends, C, Bekri, S, Bellaire, B, Bendall, LJ, Benetti, L, Berliocchi, L, Bernardi, H, Bernassola, F, Besteiro, S, Bhatia-Kissova, I, Bi, X, Biard-Piechaczyk, M, Blum, JS, Boise, LH, Bonaldo, P, Boone, DL, Bornhauser, BC, Bortoluci, KR, Bossis, I, Bost, F, Bourquin, JP, Boya, P, Boyer-Guittaut, M, Bozhkov, PV, Brady, NR, Brancolini, C, Brech, A, Brenman, JE, Brennand, A, Bresnick, EH, Brest, P, Bridges, D, Bristol, ML, Brookes, PS, Brown, EJ, Brumell, JH, et al. (2012). Guidelines for the use and interpretation of assays for monitoring autophagy. Autophagy 8:445-544

Kroemer, G (2015). Autophagy: a druggable process that is deregulated in aging and human disease. J Clin Invest 125:1-4

Laing, JG, Beyer, EC (1995). The gap junction protein connexin43 is degraded via the ubiquitin proteasome pathway. J Biol Chem 270:26399-403

Laing, JG, Tadros, PN, Westphale, EM, Beyer, EC (1997). Degradation of connexin43 gap junctions involves both the proteasome and the lysosome. Exp Cell Res 236:482-92

Lichtenstein, A, Minogue, PJ, Beyer, EC, Berthoud, VM (2011). Autophagy: a pathway that contributes to connexin degradation. J Cell Sci 124:910-20

Menzies, FM, Fleming, A, Rubinsztein, DC (2015). Compromised autophagy and neurodegenerative diseases. Nat Rev Neurosci 16:345-57

Nielsen, MS, Nygaard Axelsen, L, Sorgen, PL, Verma, V, Delmar, M, Holstein-Rathlou, NH (2012). Gap junctions. Compr Physiol 2:1981-2035

Orellana, JA, Shoji, KF, Abudara, V, Ezan, P, Amigou, E, Saez, PJ, Jiang, JX, Naus, CC, Saez, JC, Giaume, C (2011). Amyloid beta-induced death in neurons involves glial and neuronal hemichannels. J Neurosci 31:4962-77

Ponsaerts, R, D'hondt, C, Bultynck, G, Srinivas, SP, Vereecke, J, Himpens, B (2008). The myosin II ATPase inhibitor blebbistatin prevents thrombin-induced inhibition of intercellular calcium wave propagation in corneal endothelial cells. Invest Ophthalmol Vis Sci 49:4816-27

Ponsaerts, R, D'hondt, C, Hertens, F, Parys, JB, Leybaert, L, Vereecke, J, Himpens, B, Bultynck, G (2012). RhoA GTPase Switch Controls Cx43-Hemichannel Activity through the Contractile System. PLoS ONE 7:e42074

Ponsaerts, R, De Vuyst, E, Retamal, M, D'hondt, C, Vermeire, D, Wang, N, De Smedt, H, Zimmermann, P, Himpens, B, Vereecke, J, Leybaert, L, Bultynck, G (2010). Intramolecular loop/tail interactions are essential for connexin 43-hemichannel activity. Faseb J 24:4378-95

Reed, AM, Kolodecik, T, Husain, SZ, Gorelick, FS (2014). Low pH enhances connexin32 degradation in the pancreatic acinar cell. Am J Physiol Gastrointest Liver Physiol 307:G24-32

Rubinsztein, DC, Bento, CF, Deretic, V (2015). Therapeutic targeting of autophagy in neurodegenerative and infectious diseases. J Exp Med 212:979-90

Rubinsztein, DC, Marino, G, Kroemer, G (2011). Autophagy and aging. Cell 146:682-95

Scemes, E, Spray, DC, Meda, P (2009). Connexins, pannexins, innexins: novel roles of "hemi-channels". Pflugers Arch 457:1207-26

Su, V, Cochrane, K, Lau, AF (2012). Degradation of connexins through the proteasomal, endolysosomal and phagolysosomal pathways. J Membr Biol 245:389-400

Su, V, Lau, AF (2014). Connexins: mechanisms regulating protein levels and intercellular communication. FEBS Lett 588:1212-20

Vinken, M, Decrock, E, Leybaert, L, Bultynck, G, Himpens, B, Vanhaecke, T, Rogiers, V (2012a). Non-channel functions of connexins in cell growth and cell death. Biochim Biophys Acta 1818:2002-8

Vinken, M, Decrock, E, Vanhaecke, T, Leybaert, L, Rogiers, V (2012b). Connexin43 signaling contributes to spontaneous apoptosis in cultures of primary hepatocytes. Toxicol Sci 125:175-86

Wang, N, De Bock, M, Decrock, E, Bol, M, Gadicherla, A, Vinken, M, Rogiers, V, Bukauskas, FF, Bultynck, G, Leybaert, L (2013). Paracrine signaling through plasma membrane hemichannels. Biochim Biophys Acta 1828:35-50

Yang, Z, Klionsky, DJ (2010). Mammalian autophagy: core molecular machinery and signaling regulation. Curr Opin Cell Biol 22:124-31

Figure 1

Click here to download Figure Fig. 1.TIFF

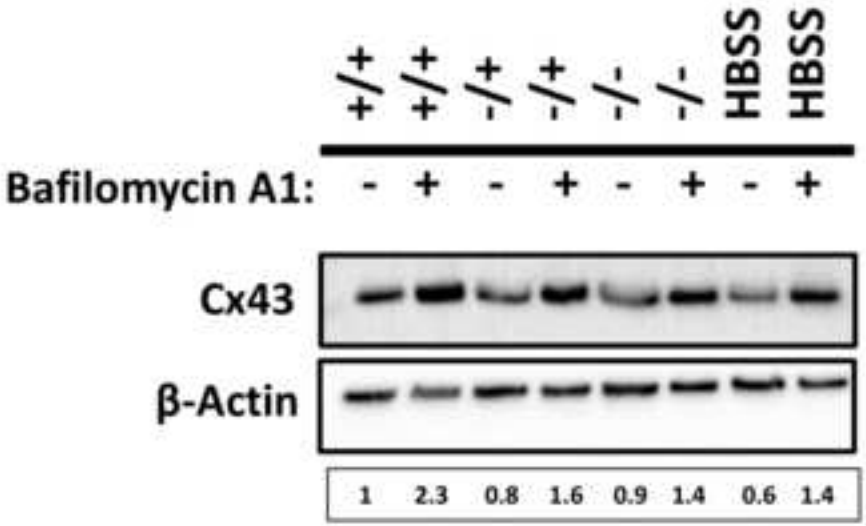

Figure 2

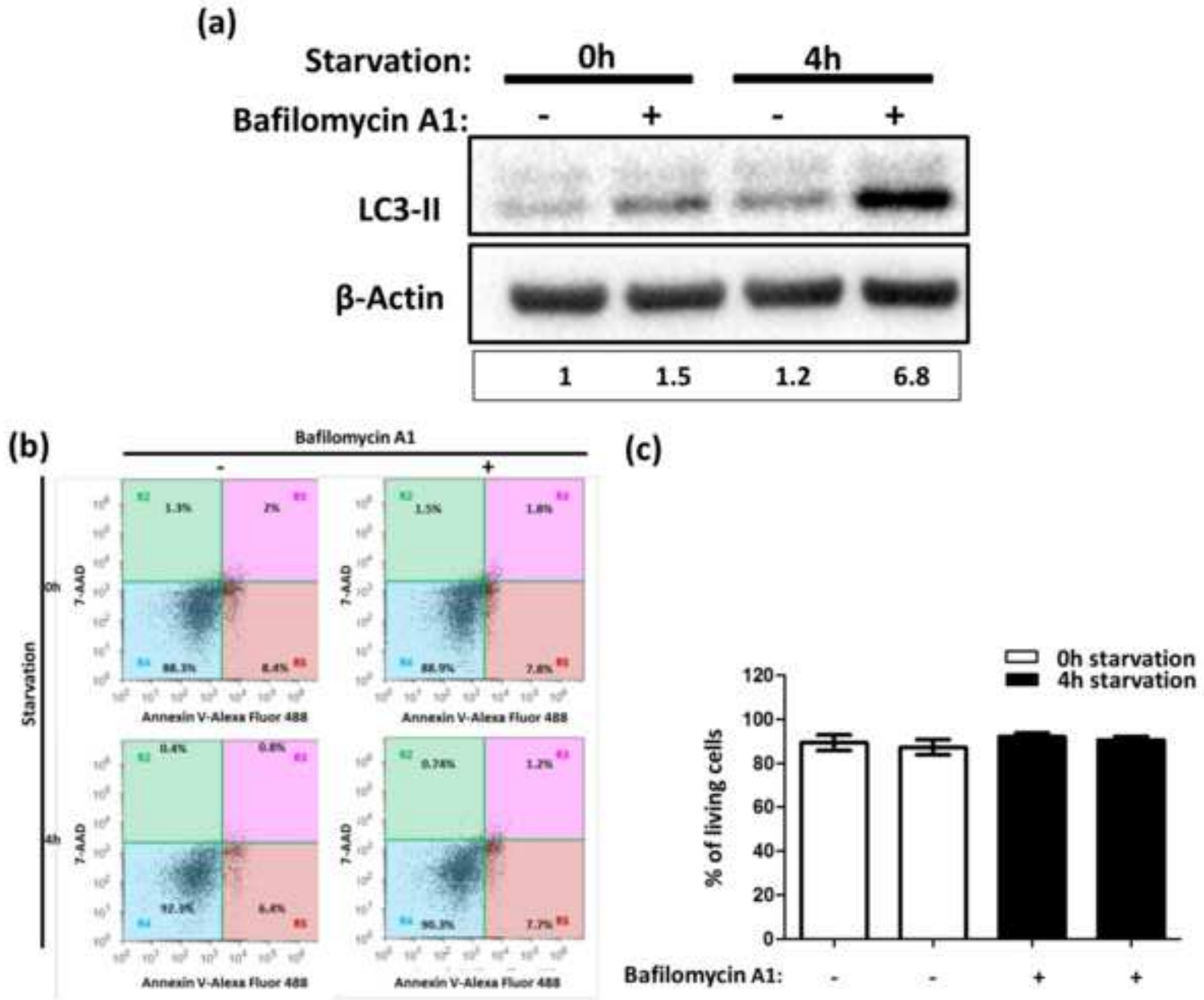

Figure 3

Click here to download Figure Fig. 3.TIFF

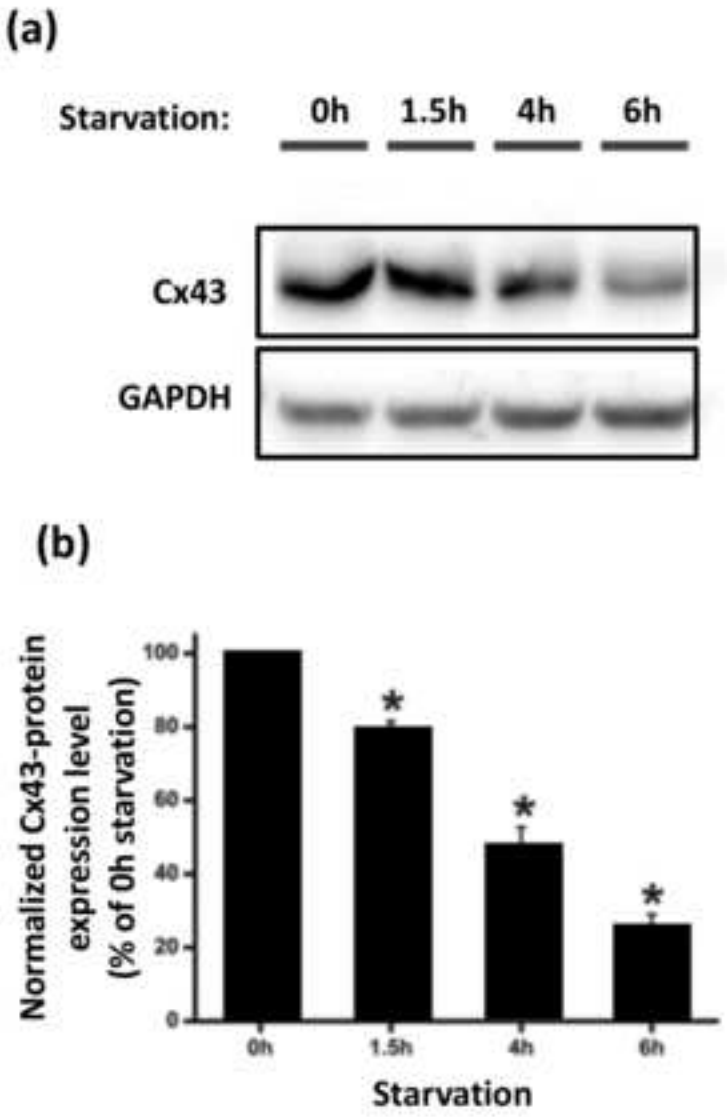

Figure 4

Click here to download Figure Fig. 4.TIFF

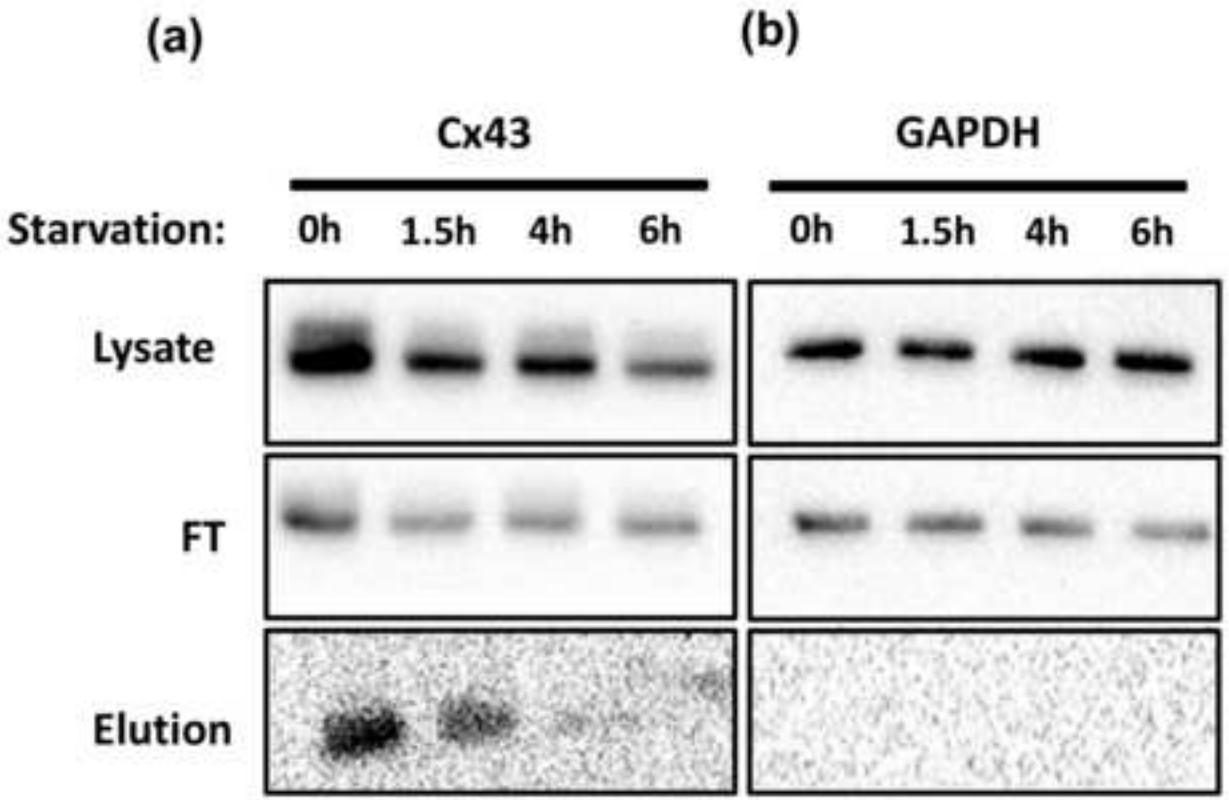

Figure 5

Click here to download Figure Fig. 5.TIFF

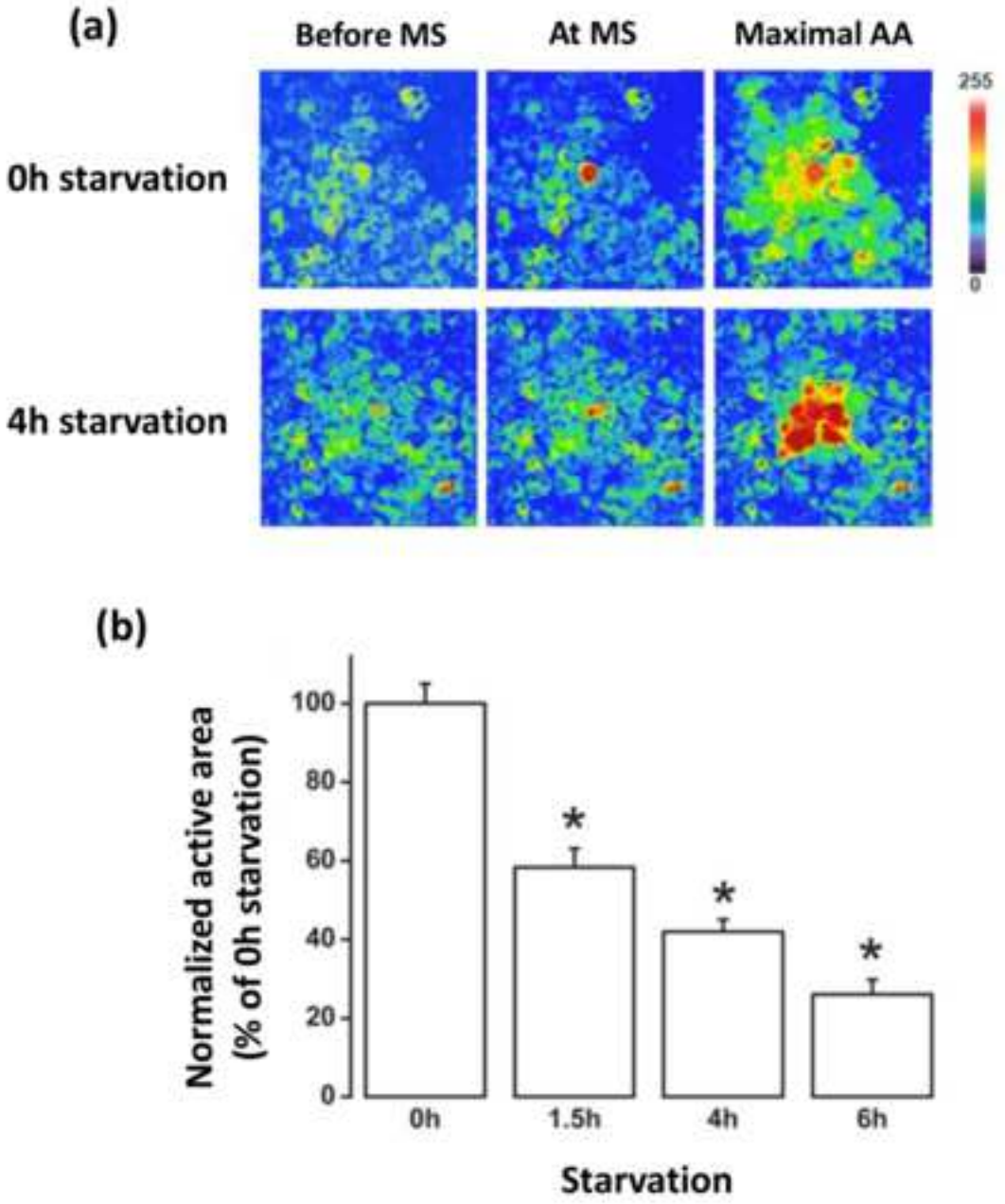

Figure 6

Click here to download Figure Fig. 6.TIFF

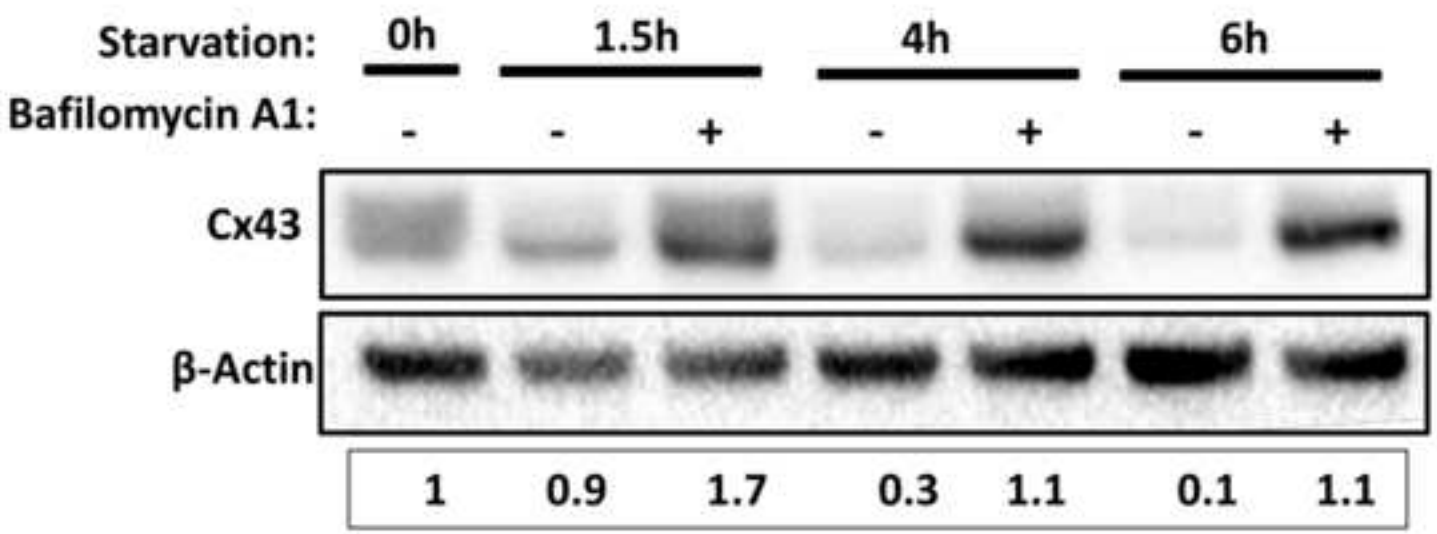

Figure 7

Click here to download Figure Fig. 7.TIFF

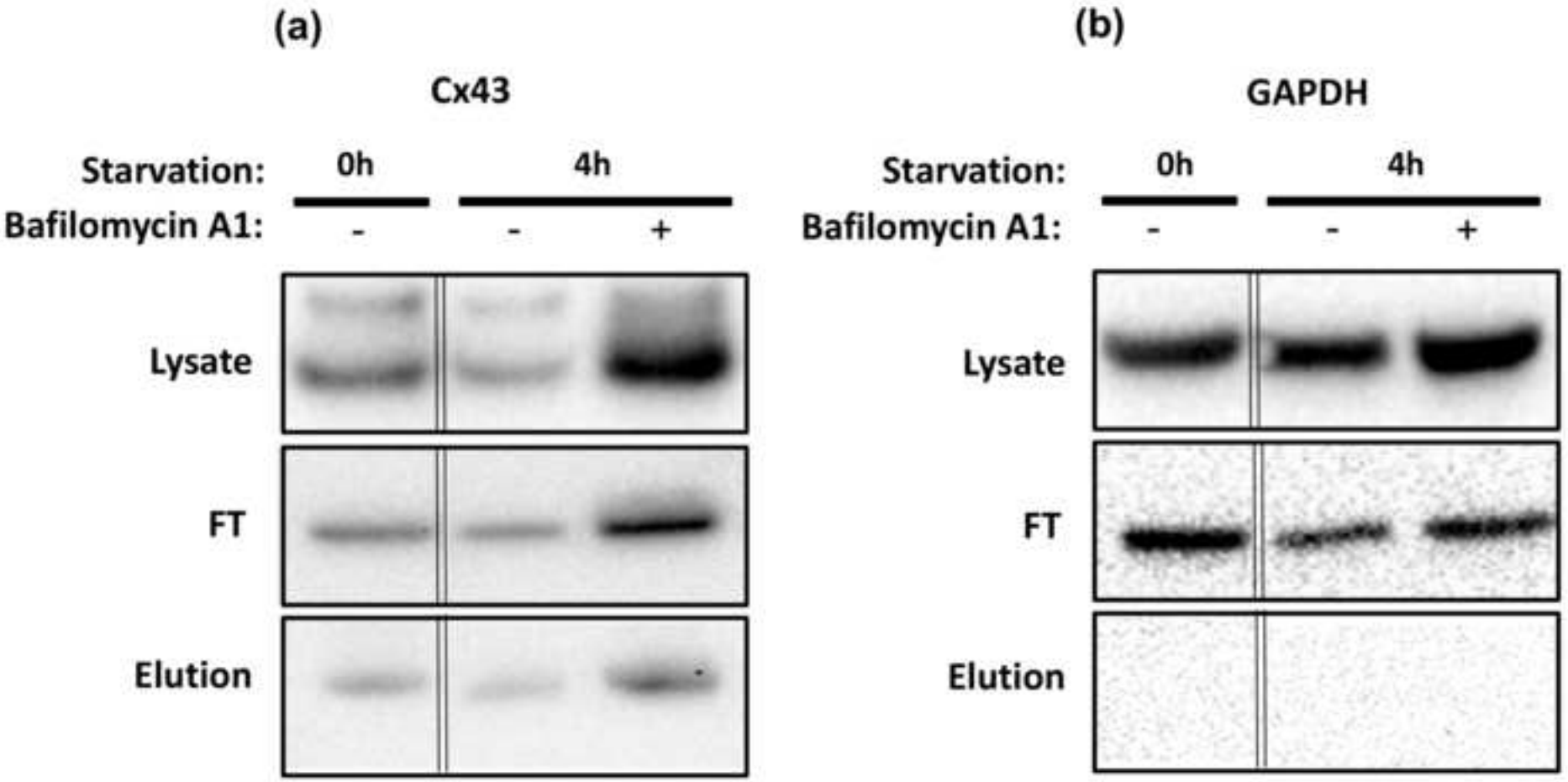

Figure 8

Click here to download Figure Fig. 8.TIFF